Journal of Sound and Vibration 333 (2014) 3536–3549

Contents lists available at ScienceDirect

Journal of Sound and Vibration

journal homepage: www.elsevier.com/locate/jsvi

# Nonlinear asymptotic impedance model for a Helmholtz resonator liner

Deepesh K. Singh, Sjoerd W. Rienstra *

*Department of Mathematics and Computer Science, Eindhoven University of Technology, 5600 MB Eindhoven, The Netherlands*

ARTICLE INFO

*Article history:*
Received 19 October 2013
Received in revised form
23 February 2014
Accepted 10 March 2014
Handling Editor: D. Juve
Available online 14 April 2014

ABSTRACT

The usual nonlinear corrections for a Helmholtz resonator type impedance do not seem to be based on a systematic asymptotic solution of the pertaining equations. We aim to present a systematic derivation of a solution of the nonlinear Helmholtz resonator equation, in order to obtain analytically expressions for impedances close to resonance, while including nonlinear effects. The amplitude regime considered is such that when we stay away from the resonance condition, the nonlinear terms are relatively small and the solution obtained is of the linear equation (formed after neglecting the nonlinear terms). Close to the resonance frequency, the nonlinear terms can no longer be neglected and algebraic equations are obtained that describe the corresponding nonlinear impedance. Sample results are presented including a few comparisons with measurements available in the literature. The validity of the model is understood in the near resonance and non-resonance regimes.



## 1. Introduction

An important type of acoustic liner for aero-engine inlet and exhaust ducts constitutes of a honeycomb array of small cells called Helmholtz resonators. The Helmholtz resonator is a cavity filled with air and having a small opening called the neck. When excited with a fluctuating external pressure, the mass of air plug inside the neck moves against the large volume of compressible air inside the cavity, which acts as a spring, while viscous forces and vortex shedding cause dissipation of energy. Altogether this establishes a mass–spring–damper system. The damping is normally relatively small such that a resonance frequency can be identified. At and near resonance, the dissipation is largest and so narrow band sound absorption is achieved for frequencies close to resonance. This process is the basic design criterion for the liners. The resonator, as "seen" from outside, is characterized by its impedance $Z=Z(\omega)$, relating (spatially averaged) pressure and velocity at the wall. Ideally, $Z$ is a wall property and independent of the acoustic field. However, in particular near resonance $Z$ is amplitude dependent for high but relevant amplitudes, for example of the "buzz saw" noise in a turbofan engine due to the shocks produced in front of the fan at take off and the blade tips operate in a supersonic regime [2,6]. Since liners are designed to operate at resonance, it is important to know quantitatively and understand qualitatively such impedances $Z$ with good precision.

The nonlinear effects are mainly of hydrodynamical origin, due to the resistive losses and vortex shedding at inflow/outflow from the opening. This is physically a process of great complexity [15,20] which has indeed exacerbated the

* Corresponding author.
*E-mail addresses:* d.k.singh@tue.nl (D.K. Singh), s.w.rienstra@tue.nl (S.W. Rienstra).

http://dx.doi.org/10.1016/j.jsv.2014.03.013
0022-460X/

possibility to obtain the impedance with an accurate model based on first principles. Ingard and Labate [23] investigated the motion of air associated with sound waves at audio frequencies in the neighbourhood of an orifice and proved a quantitative connection with the nonlinearities of the impedance of orifices. Guess [4] developed a semi-implicit method for calculating the parameters of a perforate in order to achieve a specified acoustic impedance for single-frequency excitation. Zinn [5] proposed a resistance formulation with the aid of conservation equations. Cummings and Eversman [1] demonstrated theoretically, with some approximations, that the net acoustic energy dissipation can occur when sound waves interact with free shear layers and compared the predicted and the measured net energy loss in the transmission of high amplitude impulsive acoustic waves. Hersh and Walker [13] proposed a nonlinear differential equation as a model for Helmholtz resonator response to a sound wave in the presence of grazing mean flow and provided a semi-empirical solution of the problem. The fundamental nature of their problem is the *very* high amplitude excitation of the resonator in the presence of grazing flow and hence a differential equation (slightly) different from ours. Innes and Crighton [11] gave a complete systematic solution to this model equation using matched asymptotic expansions.

In these examples, the nonlinear corrections of the impedance are based on physically inspired modelling assumptions, but otherwise do not aim to solve the equations of the nonlinear resonator [21,12,3]. In contrast, the properties of the Helmholtz resonator have been obtained from the full equations in [6–10,16,17] but these are all fully CFD, DNS or LES simulations which do not give information for the simpler models.

The present work focuses on a systematic derivation of an asymptotic solution of a stand-alone nonlinear Helmholtz resonator equation from first principles. The extra complication of grazing flow along the liner wall will not be considered here. This effect is important if the mean flow boundary layer is thin enough and the resonator outflow velocity is comparable to or higher than the mean flow velocity.

We start with the classical modelling of the Helmholtz resonator and formulate a perturbation problem in terms of a small parameter $\varepsilon$ which is based on the excitation amplitude of a given pressure of fixed frequency. The stationary solution of this problem is solved asymptotically up to second order. Secular effects of the external forcing are treated in the usual way by a suitable Lindstedt–Poincaré type transformation. A non-standard problem was the modulus term $|u|$ of the velocity. This prohibits a standard asymptotic expansion because the location of the zeros of $u$ is a priori unknown. This problem has been tackled by adding an unknown shift of the origin, to be determined along with the construction of the solution, and using the fact that the stationary solution has the same periodicity as the driving force.

## 2. Mathematical formulation

A sketch of the Helmholtz resonator considered is shown in Fig. 1. A simple and classic model (in various forms presented in the previously mentioned literature), that includes nonlinear separation effects for the air flow in and out the neck, is derived as follows. If the cross-sectional area $S_b$ of the bottle is large compared to the cross-sectional area $S_n$ of the neck, the acoustic velocities in the bottle will be small compared to those in the neck. Hence we may assume that the pressure and density perturbations $p_{\mathrm{in}}$ and $\rho_{\mathrm{in}}$ in the bottle are uniform. If the cavity neck is acoustically compact, i.e. $k\ell \ll 1$ for a typical wavenumber $k=\omega/c_0$, we can neglect compressibility in the neck and determine the line integral of the momentum equation

$$\rho_0\left(\frac{\partial \boldsymbol{v}}{\partial t}+\boldsymbol{v}\cdot\nabla\boldsymbol{v}\right)+\nabla p=\mu\nabla^2\boldsymbol{v}$$

along a typical streamline with velocity $\boldsymbol{v}$ from a point (just) inside to a point (just) outside the neck. We obtain the relation

$$\rho_0\int_{\mathrm{in}}^{\mathrm{ex}}\frac{\partial \boldsymbol{v}}{\partial t}\cdot\mathbf{ds}+\frac{1}{2}\rho_0\left(v_{\mathrm{ex}}^2-v_{\mathrm{in}}^2\right)+\left(p_{\mathrm{ex}}-p_{\mathrm{in}}\right)=\int_{\mathrm{in}}^{\mathrm{ex}}\mu\nabla^2\boldsymbol{v}\cdot\mathbf{ds}, \tag{1}$$

with $v=\|\boldsymbol{v}\|$ and $\mu$ denoting the viscosity. Following Melling [21] we average pressure and velocity along the neck's cross section, assume that the averaged squared velocity is approximately equal to the squared averaged velocity, and obtain

$$\rho_0\int_{\mathrm{in}}^{\mathrm{ex}}\frac{\partial \overline{\boldsymbol{v}}}{\partial t}\cdot\mathbf{ds}+\frac{1}{2}\rho_0\left(\overline{v}_{\mathrm{ex}}^2-\overline{v}_{\mathrm{in}}^2\right)+\left(p_{\mathrm{ex}}-p_{\mathrm{in}}\right)=\int_{\mathrm{in}}^{\mathrm{ex}}\mu\overline{\nabla^2\boldsymbol{v}}\cdot\mathbf{ds}. \tag{2}$$

Assuming that the streamline does not change in time, we have

$$\int_{\mathrm{in}}^{\mathrm{ex}}\frac{\partial \overline{\boldsymbol{v}}}{\partial t}\cdot\mathbf{ds}=\frac{\mathrm{d}}{\mathrm{d}t}\int_{\mathrm{in}}^{\mathrm{ex}}\overline{\boldsymbol{v}}\cdot\mathbf{ds}. \tag{3}$$

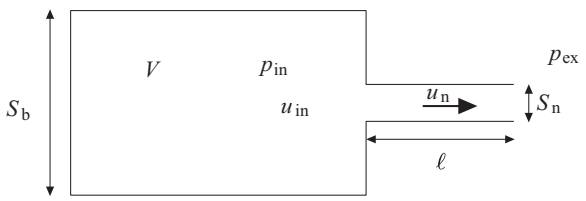


**Fig. 1.** Helmholtz resonator.

The velocity line integral evidently scales on a typical length times a typical velocity. If end effects are minor, we can use the neck flux velocity $\overline{\boldsymbol{v}} = u_n \boldsymbol{e}_x$ with a corresponding length being the neck length $\ell$, added by a small end correction $\delta$ to take into account the inertia of the acoustic flow at both ends just outside the neck (inside and outside the resonator). Then we have

$$\int_{\text{in}}^{\text{ex}} \overline{\boldsymbol{v}} \cdot \mathbf{ds} = (\ell + 2\delta) u_n. \tag{4}$$

End corrections $\delta$ for various geometries are given by Ingard [14]. For a circular orifice, for example, we may use

$$\delta = 0.85 \left(\frac{S_n}{\pi}\right)^{1/2}, \tag{5}$$

although one should be aware of the fact that this suggests an accuracy, totally incompatible with the modelling assumptions necessary for (4).

For the stress term line integral we observe that, apart from $u_n$ itself, it will depend on flow profile, Reynolds number, wall heat exchange, turbulence, separation from sharp edges, and maybe more. Following Melling [21], we will take these effects together in a resistance factor $R$, which will be assumed relatively small, in order to have resonance and a small decay per period to begin with. We thus have

$$\int_{\text{in}}^{\text{ex}} \mu \overline{\nabla^2 \boldsymbol{v}} \cdot \mathbf{ds} = -R u_n. \tag{6}$$

(Note that this form is exact for a Poiseuille flow with parabolic profile.) Due to separation from the outer exit, we have with outflow $\overline{v}_{\text{in}} \simeq 0$ with $\overline{v}_{\text{ex}} = u_n$ jetting out, while similarly during inflow, $\overline{v}_{\text{ex}} \simeq 0$ with $\overline{v}_{\text{in}} = u_n$ jetting into the cavity; see Fig. 2. The pressure in the jets, however, has to remain equal to the surrounding pressure ($p_{\text{ex}}$ and $p_{\text{in}}$ respectively) because the boundary of the jet cannot support a pressure difference. Therefore, we have altogether

$$\rho_0(\ell + 2\delta)\frac{\mathrm{d}}{\mathrm{d}t}u_n + \frac{1}{2}\rho_0 u_n |u_n| + R u_n = p_{\text{in}} - p_{\text{ex}}. \tag{7}$$

The second equation between $p_n$ and $u_n$ is obtained by applying the integral mass conservation law on the volume $V$ of the cavity. The change of mass must be equal to the flux through the cavity neck, which is in linearised form for the density perturbation $\rho_{\text{in}}$

$$V\frac{\mathrm{d}\rho_{\text{in}}}{\mathrm{d}t} = -\rho u_n S_n \approx -\rho_0 u_n S_n. \tag{8}$$

Assuming an adiabatic compression of the fluid in the cavity, we have $p_{\text{in}} = c_0^2 \rho_{\text{in}}$. Elimination of $\rho_{\text{in}}$ and $u_n$ from (7) by using (8) and redefining $(\ell + 2\delta) =: \ell$ yields the nonlinear Helmholtz resonator equation:

$$\frac{\ell V}{c_0^2 S_n}\frac{\mathrm{d}^2 p_{\text{in}}}{\mathrm{d}t^2} + \frac{V^2}{2\rho_0 c_0^4 S_n^2}\frac{\mathrm{d}p_{\text{in}}}{\mathrm{d}t}\left|\frac{\mathrm{d}p_{\text{in}}}{\mathrm{d}t}\right| + \frac{RV}{\rho_0 c_0^2 S_n}\frac{\mathrm{d}p_{\text{in}}}{\mathrm{d}t} + p_{\text{in}} = p_{\text{ex}}. \tag{9}$$

For a proper analysis it is most clarifying to rewrite the equation into non-dimensional variables. For this we need an inherent timescale and pressure level. For vanishing amplitudes and negligible dissipation the equation describes a harmonic oscillator, so the reciprocal of its angular frequency

$$\omega_0 = \frac{c_0}{\ell}\left(\frac{\ell S_n}{V}\right)^{1/2}$$

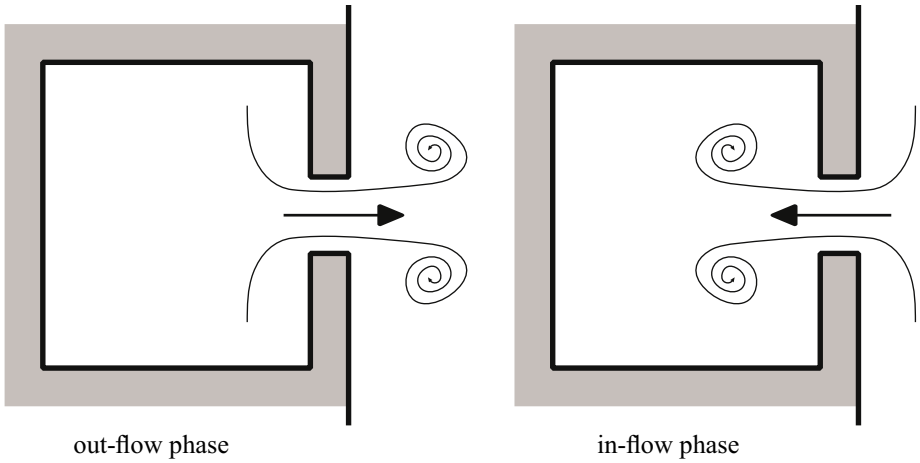


**Fig. 2.** Separation and vortex shedding during the out-flow and the in-flow phase.

is a suitable timescale of the problem. By dividing the nonlinear damping term by the acceleration term we find the pressure level $2\rho_0 c_0^2 \ell S_n/V$ at which the nonlinear damping would be just as large as the other terms. So for a pressure that is a small fraction, say $\varepsilon$, of this level we have a problem with only little nonlinear damping. In addition we assume that the linear damping is small and of the same order of magnitude as the nonlinear damping (that is to say: near resonance. Away from resonance the nonlinear term will be relatively smaller). Also, the driving amplitude $p_{ex}$ will be an order smaller than $p_{in}$. In order to make all this explicit we introduce a small parameter $\varepsilon$ (via the external forcing amplitude), and make dimensionless

$$\tau=\omega_0 t,\quad p_{in}=2\varepsilon\rho_0 c_0^2\left(\frac{\ell S_n}{V}\right)y,\quad p_{ex}=2\varepsilon^2\rho_0 c_0^2\left(\frac{\ell S_n}{V}\right)F,\quad R=\varepsilon\rho_0 c_0\left(\frac{\ell S_n}{V}\right)^{1/2}r, \tag{10}$$

where $0<\varepsilon\ll 1$ and $r,y,F=O(1)$.

Suppose that we excite the Helmholtz resonator harmonically, such that $p_{ex}=C\cos(\omega t)+H(t)$ consists of a time-harmonic component of frequency $\omega$ plus a small contribution of higher harmonics $H$ due to the interaction with the resonator.[1] In the scaled variables $\tau$ and $F$ this becomes

$$F=F_0\cos(\Omega\tau)+\varepsilon^\nu h(\tau),\quad \Omega=\frac{\omega}{\omega_0}, \tag{11}$$

where $\nu=1$ in the resonant case and $\nu=2$ in the non-resonant case.

Note that $\varepsilon$ is a bookkeeping parameter, meant to measure the "smallness" of the various parameters and variables. In practice it is determined by the external forcing $p_{ex}$, so in the simple case of a harmonic excitation we can take $F_0=1$, and this will be done in any example below. Hence we have, for a case with harmonic excitation at a pressure level given by *SPL* dB, an equivalent value of $\varepsilon$ given by

$$\varepsilon=\left(\frac{2\times 10^{-5}\times 10^{\mathrm{SPL}/20}}{2\rho_0 c_0^2\frac{\ell S_n}{V}\frac{1}{2}\sqrt{2}}\right)^{1/2}. \tag{12}$$

Finally we arrive at the weakly nonlinear forced oscillator as given by (13). The initial conditions are not important as we are interested only in the stationary state[2] of the oscillator synchronised with the forcing

$$\frac{\mathrm{d}^2y}{\mathrm{d}\tau^2}+\varepsilon\frac{\mathrm{d}y}{\mathrm{d}\tau}\left|\frac{\mathrm{d}y}{\mathrm{d}\tau}\right|+\varepsilon r\frac{\mathrm{d}y}{\mathrm{d}\tau}+y=\varepsilon F_0\cos(\Omega\tau)+\varepsilon^{1+\nu}h(\tau). \tag{13}$$

We note in passing that the problem considered by Innes and Crighton [11] relates to ours if we replace $y'|y'|$ by $y'|y|$, assume $y=O(\varepsilon^{-2})$ and $F=O(\varepsilon^{-4})$, and neglect $r$.

## 3. Asymptotic analysis

### 3.1. Non-resonant case

Away from resonance, when $1-\Omega^2=O(1)$, the perturbation problem is regular and relatively straightforward. We will include it here for reference.

We look for solutions of

$$y''+\varepsilon y'|y'|+\varepsilon r y'+y=\varepsilon F_0\cos(\Omega\tau)+\varepsilon^3 h(\tau) \tag{14}$$

that are only caused by the external forcing. Since this forcing term is $O(\varepsilon)$ and we are not near resonance, the response is of the same order of magnitude, and we transform $y=\varepsilon Y$, where $Y=O(1)$

$$Y''+\varepsilon^2 Y'|Y'|+\varepsilon r Y'+Y=F_0\cos(\Omega\tau)+\varepsilon^2 h(\tau). \tag{15}$$

After substituting the assumed expansion $Y(\tau;\varepsilon)=Y_0(\tau)+\varepsilon Y_1(\tau)+\varepsilon^2 Y_2(\tau)+\cdots$ and collecting the coefficients of $O(1)$, we have

$$Y_0''+Y_0=F_0\cos(\Omega\tau). \tag{16}$$

The solution that follows the driving force is periodic with frequency $\Omega$ and so

$$Y_0=\frac{F_0}{1-\Omega^2}\cos(\Omega\tau), \tag{17}$$

[1] $H$ will play no role in the results, but appears from the liner application of Section 5. Here, the external forcing field is a combination of incident and reflected waves, say $p_{ex}=f(t)+g(t)$ and $v_{ex}\propto f(t)-g(t)$. If incident part $f$ is harmonic, reflected part $g$ will be harmonic plus higher harmonics. We will see, however, that these higher harmonics are one or two orders of magnitude smaller, and therefore play no role in $y_1$, Eq. (34), respectively $Y_1$, Eq. (19).

[2] In the appendix it is proved that solutions of Eq. (13) are stable, so the stationary solution exists.

Next we collect the coefficients of $O(\varepsilon)$ to obtain

$$Y_1'' + Y_1 = -rY_0' = \frac{rF_0\Omega}{1-\Omega^2}\ \sin(\Omega\tau) \tag{18}$$

with solution

$$Y_1 = \frac{rF_0\Omega}{(1-\Omega^2)^2}\ \sin(\Omega\tau). \tag{19}$$

We may go on to $O(\varepsilon^2)$ and find the appearance of higher harmonics. Efficiently collecting terms together, we obtain for the full solution

$$y = \varepsilon F_0 \frac{(1-\Omega^2)\ \cos\ \Omega\tau + \varepsilon r\Omega\ \sin\ \Omega\tau}{(1-\Omega^2)^2 + \varepsilon^2 r^2\Omega^2} + O(\varepsilon^3) \tag{20}$$

showing that the response is indeed $O(\varepsilon)$ and follows the excitation almost in phase ($1-\Omega^2 > 0$) or anti-phase ($1-\Omega^2 < 0$). This is not the case anymore near resonance when $1-\Omega^2 = O(\varepsilon)$.

### 3.2. Resonant case

Near resonance when $1-\Omega^2 = O(\varepsilon)$, it was assumed and indeed confirmed by (20) that the amplitude $y$ rises to levels of $O(1)$, and the assumption that the nonlinear damping is negligible to leading orders is not correct. As the physics of the problem essentially changes when $\Omega = 1 + O(\varepsilon)$, we introduce a parameter $\sigma = O(1)$ and assume that

$$\Omega = 1 + \varepsilon\sigma. \tag{21}$$

However, posed in this form we obtain secular terms in the expansion $\cos(\tau+\varepsilon\sigma\tau) = \cos(\tau) - \varepsilon\sigma\tau\ \sin(\tau) + \cdots$ of the driving force, which prohibits a uniform approximation of $y$ later [19, Section 15.3.2]. Therefore we remove the $\varepsilon$-dependence from the driving force by absorbing $\Omega$ into a new time coordinate.

Moreover, the asymptotic expansion of the modulus $|y'|$ introduces difficulties near the $\varepsilon$-dependent (and unknown) zeros of $y'$. This will be tackled by a translation of the origin by an amount $\theta(\varepsilon)$, such that the locations of the sign change of $y'$ are fixed (as $y$ is synchronised with the driving force) and independent of $\varepsilon$. (Of course, a certain amount of smoothness is anticipated such that $y'$ has the same number of zeros per period as the forcing term.) So we introduce

$$\tilde{\tau} = \Omega\tau - \theta(\varepsilon)$$

to obtain

$$\Omega^2\frac{\mathrm{d}^2y}{\mathrm{d}\tilde{\tau}^2} + \varepsilon\Omega^2\frac{\mathrm{d}y}{\mathrm{d}\tilde{\tau}}\left|\frac{\mathrm{d}y}{\mathrm{d}\tilde{\tau}}\right| + \varepsilon\Omega r\frac{\mathrm{d}y}{\mathrm{d}\tilde{\tau}} + y = \varepsilon F_0\ \cos(\tilde{\tau}+\theta) + \varepsilon^2 h, \tag{22}$$

where $\theta$ is to be chosen such that $y'(\tilde{\tau}) = 0$ at $\tilde{\tau} = N\pi$. In other words, $\Omega\tau = \omega t = \theta$ corresponds with the phase lag of response $p_{\mathrm{in}}$ to excitation $p_{\mathrm{ex}}$.

When we substitute the following (assumed uniform) asymptotic expansions for $y$ and $\theta$ [18]:

$$y(\tilde{\tau};\varepsilon) = y_0(\tilde{\tau}) + \varepsilon y_1(\tilde{\tau}) + \varepsilon^2 y_2(\tilde{\tau}) + \cdots \quad \text{and} \quad \theta(\varepsilon) = \theta_0 + \varepsilon\theta_1 + \cdots,$$

and collect like powers of $\varepsilon$, we find for $y_0$

$$\frac{\mathrm{d}^2y_0}{\mathrm{d}\tilde{\tau}^2} + y_0 = 0, \quad y_0'(N\pi) = 0. \tag{23}$$

This has the general solution

$$y_0(\tilde{\tau}) = A_0\ \cos(\tilde{\tau}), \tag{24}$$

with $A_0$ and $\theta_0$ to be determined. Although $y_0$ is the result of driving force $F$, at this level we do not have any information about their relation yet, so we cannot determine the integration constants $A_0$ and $\theta_0$. Therefore, we continue with the next order $y_1$.

$$\begin{aligned}\frac{\mathrm{d}^2y_1}{\mathrm{d}\tilde{\tau}^2} + y_1 &= F_0\ \cos(\tilde{\tau}+\theta_0) - 2\sigma\frac{\mathrm{d}^2y_0}{\mathrm{d}\tilde{\tau}^2} - \frac{\mathrm{d}y_0}{\mathrm{d}\tilde{\tau}}\left|\frac{\mathrm{d}y_0}{\mathrm{d}\tilde{\tau}}\right| - r\frac{\mathrm{d}y_0}{\mathrm{d}\tilde{\tau}} \\ &= F_0\ \cos(\tilde{\tau}+\theta_0) + 2\sigma A_0\ \cos(\tilde{\tau}) + A_0|A_0|\sin(\tilde{\tau})\left|\sin(\tilde{\tau})\right| + rA_0\ \sin(\tilde{\tau})\end{aligned} \tag{25}$$

From the arguments that $y$ is the stationary solution and its asymptotic expansion is uniform in $\tilde{\tau}$, it follows that no resonant excitation is allowed on the right hand side of the equation for $y_1$. This means that we should suppress the cos- and sin-terms, including the first term of the Fourier expansion of

$$\sin(\tilde{\tau})\left|\sin(\tilde{\tau})\right| = -\frac{1}{\pi}\sum_{n=0}^{\infty}\frac{\sin(2n+1)\tilde{\tau}}{\left(n^2-\frac{1}{4}\right)\left(n+\frac{3}{2}\right)} = \frac{8}{3\pi}\ \sin\ \tilde{\tau} + \cdots \tag{26}$$

to obtain

$$F_0\ \cos\ \theta_0 = -2\sigma A_0, \quad F_0\ \sin\ \theta_0 = \left(\frac{8}{3\pi}|A_0|+r\right)A_0 \tag{27}$$

or

$$\left[\left(\frac{8}{3\pi}|A_0|+r\right)^2+(2\sigma)^2\right]A_0^2 = F_0^2, \quad \tan(\theta_0) = -\frac{\frac{8}{3\pi}|A_0|+r}{2\sigma}. \tag{28}$$

In general, the equation for $A_0$ has to be solved numerically, from which $\theta_0$ follows. There exist two (real) solutions, while if $(A_0,\theta_0)$ is a solution, then also $(-A_0,\theta_0+\pi)$. So, if convenient, we could assume that $A_0$ is positive and maintain $|A_0|=A_0$, but this depends on $\theta_0$.

The next order $y_1$ is then given by

$$y_1(\tilde\tau) = A_1\ \cos\ \tilde\tau + B_1\ \sin\ \tilde\tau + \frac{1}{4\pi}A_0|A_0|\sum_{n=1}^{\infty}\frac{\sin(2n+1)\tilde\tau}{n(n+1)\left(n^2-\frac{1}{4}\right)\left(n+\frac{3}{2}\right)} \tag{29}$$

with derivative

$$y_1'(\tilde\tau) = -A_1\ \sin\tilde\tau + B_1\ \cos\ \tilde\tau + \frac{1}{4\pi}A_0|A_0|\sum_{n=1}^{\infty}\frac{(2n+1)\ \cos(2n+1)\tilde\tau}{n(n+1)\left(n^2-\frac{1}{4}\right)\left(n+\frac{3}{2}\right)} \tag{30}$$

and so the boundary condition

$$\begin{aligned} y_1'(N\pi) &= -A_1\ \sin(N\pi) + B_1\ \cos(N\pi) + \frac{1}{4\pi}A_0|A_0|\sum_{n=1}^{\infty}\frac{(2n+1)\ \cos((2n+1)N\pi)}{n(n+1)\left(n^2-\frac{1}{4}\right)\left(n+\frac{3}{2}\right)} \\ &= (-1)^N B_1 + \frac{(-1)^N}{4\pi}A_0|A_0|\sum_{n=1}^{\infty}\frac{2n+1}{n(n+1)\left(n^2-\frac{1}{4}\right)\left(n+\frac{3}{2}\right)} = (-1)^N\left[B_1+\frac{2}{9\pi}A_0|A_0|\right] = 0 \end{aligned} \tag{31}$$

is satisfied by

$$B_1 = -\frac{2}{9\pi}A_0|A_0| \quad \text{because} \quad \sum_{n=1}^{\infty}\frac{2n+1}{n(n+1)\left(n^2-\frac{1}{4}\right)\left(n+\frac{3}{2}\right)} = \frac{8}{9}.$$

The sum of the telescoping series is easily found by partial fractions and noting the terms cancelling in pairs. Altogether we have

$$y_1(\tilde\tau) = A_1\ \cos\ \tilde\tau - \frac{2}{9\pi}A_0|A_0|\ \sin\ \tilde\tau + \frac{1}{4\pi}A_0|A_0|\sum_{n=1}^{\infty}\frac{\sin(2n+1)\tilde\tau}{n(n+1)\left(n^2-\frac{1}{4}\right)\left(n+\frac{3}{2}\right)}. \tag{32}$$

The amplitude $A_1$ is to be determined in a similar way as with $y_0$ by suppressing resonant terms in $y_2$. The next order term $y_2$ is obtained from (22) when it is expanded to $O(\varepsilon^2)$ and terms of $O(\varepsilon^2)$ are collected

$$y_2''+y_2 = -\sigma^2 y_0'' - 2\sigma y_1'' - 2\sigma y_0'|y_0'| - 2y_1'|y_0'| - ry_1' - r\sigma y_0' - \theta_1 F_0\ \sin(\tilde\tau+\theta_0) + h. \tag{33}$$

After substituting $y_0$ and $y_1$, and considering only the terms on the right hand side that are possibly in resonance with the left hand side, we obtain

$$\begin{aligned} y_2''+y_2 &= \sigma^2 A_0\ \cos\ \tilde\tau + 2\sigma A_1\ \cos\ \tilde\tau - \frac{4}{9\pi}\sigma A_0|A_0|\ \sin\ \tilde\tau \\ &+ \left(2\sigma A_0\ \sin\ \tilde\tau + 2A_1\ \sin\tilde\tau + \frac{4}{9\pi}A_0|A_0|\ \cos\ \tilde\tau - \frac{1}{\pi}A_0|A_0|\sum_{n=1}^{\infty}\frac{\cos(2n+1)\tilde\tau}{n(n+1)\left(n-\frac{1}{2}\right)\left(n+\frac{3}{2}\right)}\right)|A_0\ \sin\tilde\tau| \\ &+ rA_1\ \sin\ \tilde\tau + \frac{2}{9\pi}rA_0|A_0|\ \cos\ \tilde\tau + r\sigma A_0\ \sin\ \tilde\tau - \theta_1 F_0\ \cos\ \theta_0\ \sin\ \tilde\tau - \theta_1 F_0\ \sin\ \theta_0\ \cos\ \tilde\tau + \cdots \end{aligned} \tag{34}$$

By Fourier expansion it can be found that

$$\cos\ \tilde\tau|\sin\ \tilde\tau| = \frac{4}{3\pi}\cos\ \tilde\tau + \cdots, \quad \sum_{n=1}^{\infty}\frac{|\sin\ \tilde\tau|\ \cos(2n+1)\tilde\tau}{n(n+1)\left(n-\frac{1}{2}\right)\left(n+\frac{3}{2}\right)} = \frac{1}{\pi}\left(\frac{80}{27}-\frac{\pi^2}{3}\right)\ \cos\ \tilde\tau + \cdots \tag{35}$$

and only higher harmonics otherwise. Suppressing the cos- and sin-terms of (34) thus results in

$$\begin{aligned} 2\sigma A_1 - \theta_1 F_0\ \sin\ \theta_0 &= -\sigma^2 A_0 - \left(\frac{1}{3}-\frac{64}{27\pi^2}\right)A_0^3 - \frac{2}{9\pi}rA_0|A_0|, \\ \left(\frac{16}{3\pi}|A_0|+r\right)A_1 - \theta_1 F_0\ \cos\ \theta_0 &= -\left(\frac{44}{9\pi}|A_0|+r\right)\sigma A_0. \end{aligned} \tag{36}$$

By solving the linear system (36), we can obtain $A_1$ and $\theta_1$.

## 4. Time-domain solution

The solution $y = y_0 + \varepsilon y_1 + O(\varepsilon^2)$ ascertains in principle (for small $\varepsilon$) a better approximation of $y$ than the leading order approximation $y_0$, which would later provide a better approximation of the impedance. We have this full solution as

$$y(\tilde{\tau};\varepsilon) = (A_0 + \varepsilon A_1)\ \cos\ \tilde{\tau} - \frac{2}{9\pi}\varepsilon A_0|A_0|\ \sin\ \tilde{\tau} + \frac{1}{4\pi}\varepsilon A_0|A_0| \sum_{n=1}^{\infty} \frac{\sin(2n+1)\tilde{\tau}}{n(n+1)\left(n^2-\frac{1}{4}\right)\left(n+\frac{3}{2}\right)} + \cdots. \tag{37}$$

where $\tilde{\tau} = \omega t - \theta$ and $\theta = \theta_0 + \varepsilon\theta_1 + \cdots$. The constants $A_0$, $\theta_0$ and $A_1$, $\theta_1$ can be determined from (27) and (36) respectively.

Consider first the leading order approximation. Eq. (28) for $A_0$ has two real symmetric solutions (of which we normally need to consider only the positive one), but solving $A_0 = A_0(\sigma)$ is not straightforward. Therefore, it is useful to consider the inverse, $\sigma = \sigma(A_0)$, given by

$$4\sigma^2 = \frac{F_0^2}{A_0^2} - \left(\frac{8}{3\pi}|A_0| + r\right)^2 \tag{38}$$

Since $\sigma^2 \geq 0$ we see immediately that solutions exist only for a finite interval in $A_0$, while $\sigma \to \infty$ only when $A_0 \to 0$. In particular, we have

$$A_0 \simeq \frac{F_0}{2|\sigma|}, \quad \tan\ \theta_0 \simeq -\frac{r}{2\sigma} \quad \text{or} \quad \theta_0 \simeq -\frac{r}{2\sigma} + n\pi, \tag{39}$$

which is in exact agreement with the asymptotic behaviour for $\Omega = 1 + \varepsilon\sigma$, $\sigma$ large, corresponding to the linear solution (17). In fact, by tracing the solution parametrically as a function of $\sigma$, we can see that if we start with $\theta_0 = 0$ for $\sigma \to -\infty$, we end with $\theta_0 = \pi$ for $\sigma \to \infty$. In this way, we have obtained the expression for $A_0$ and $\theta_0$; see Fig. 3 for an example.

Substituting the obtained value of $A_0$ and $\theta_0$ in (36), we can solve the linear algebraic system to obtain $A_1$ and $\theta_1$. This way, we have determined all the coefficients in (37); hence, the solution $y$ is known which, when used with (10), gives $p_{\text{in}}$

$$p_{\text{in}} = 2\varepsilon\rho_0 c_0^2 \frac{\ell S_n}{V}\left[(A_0 + \varepsilon A_1)\ \cos(\omega t - \theta) - \frac{2}{9\pi}\varepsilon A_0|A_0|\ \sin(\omega t - \theta) + \frac{1}{4\pi}\varepsilon A_0|A_0| \sum_{n=1}^{\infty} \frac{\sin(2n+1)(\omega t-\theta)}{n(n+1)\left(n^2-\frac{1}{4}\right)\left(n+\frac{3}{2}\right)} + \cdots\right]. \tag{40}$$

From this solution and (8) we may determine the neck velocity $u_n$

$$u_n = 2\varepsilon\omega\ell\left[(A_0 + \varepsilon A_1)\ \sin(\omega t - \theta) + \frac{2}{9\pi}\varepsilon A_0|A_0|\ \cos(\omega t - \theta) - \frac{1}{4\pi}\varepsilon A_0|A_0| \sum_{n=1}^{\infty} \frac{(2n+1)\ \cos(2n+1)(\omega t-\theta)}{n(n+1)\left(n^2-\frac{1}{4}\right)\left(n+\frac{3}{2}\right)} + \cdots\right], \tag{41}$$

which will be used to obtain the impedance of the resonator in the later section.

### 4.1. Comparison in time-domain with a fully numerical solution

The solution (37), correct till $O(\varepsilon)$ ($y_0$) and $O(\varepsilon^2)$ ($y_0 + \varepsilon y_1$), is compared with a fully numerical solution of (13), obtained by Mathematica with a standard Runge–Kutta routine, see Fig. 4. In both cases $r = 0.2$, $\sigma = 1$, while $\varepsilon = 0.28$ in the left figure and $\varepsilon = 0.88$ in the right. Note that this last case is added to see how the solution behaves for values of $\varepsilon$ that are really not small anymore. The one with $\varepsilon = 0.28$ is indeed remarkably accurate for $y_0 + \varepsilon y_1$, and we may observe an error of $y_0$ and $y_0 + \varepsilon y_1$ compared to $y$ that follows indeed the predicted behaviour of $O(\varepsilon)$ and $O(\varepsilon^2)$. The one with $\varepsilon = 0.88$ cannot be expected to be really accurate, but surprisingly the results are still of the right order of magnitude.

We note, however, that there is always the assumption that $\sigma = O(1)$ and $1 - \Omega^2 = O(\varepsilon)$. In other words, the validity of the resonance solution is for an interval in frequency of $\omega = \omega_0(1 + O(\varepsilon))$. When we leave this interval, the non-resonant solution (20) should gradually become applicable.

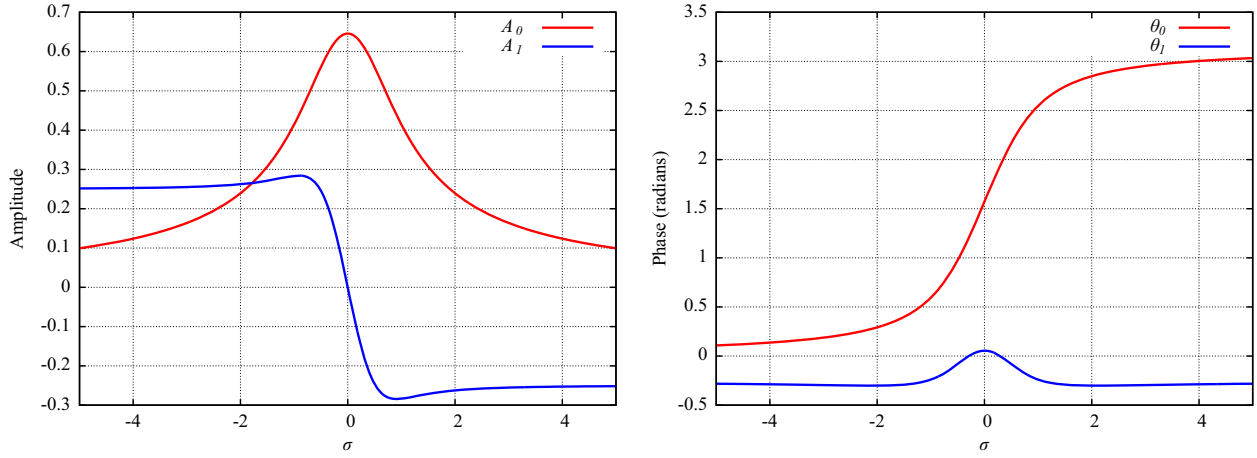


**Fig. 3.** Solution of amplitude ($A_0$, $A_1$) and phase ($\theta_0$ , $\theta_1$) as a function of $\sigma$, while $r = F_0 = 1$.

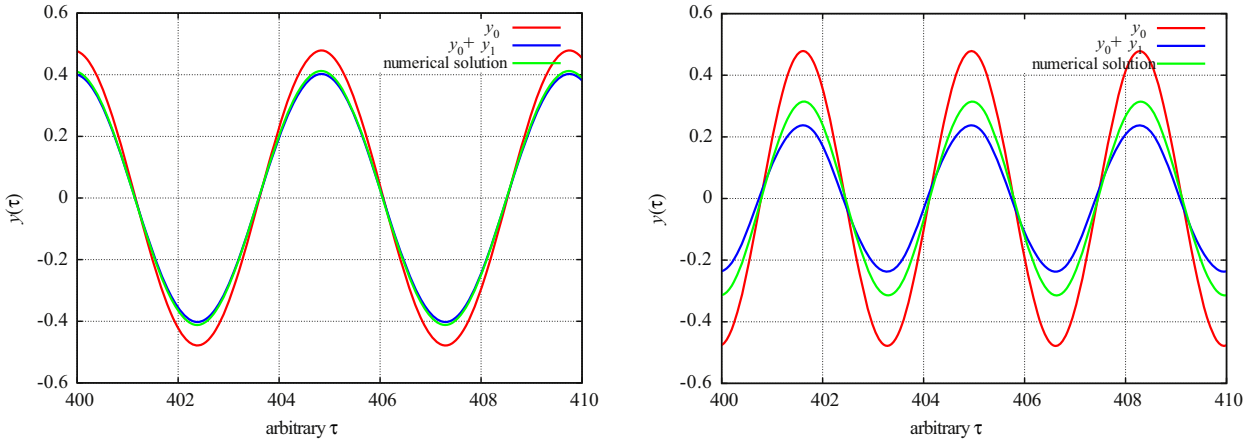


**Fig. 4.** Comparison of solution $y_0$ and $y_0+\varepsilon y_1$ for $r=0.2$, $\sigma=1$ and $\varepsilon=0.28$ (left) and $\varepsilon=0.88$ (right) with a fully numerical solution.

## 5. Impedance calculation

In order to obtain realistic numbers, we will consider the impedance $Z$ as the effective impedance of an array of Helmholtz resonators, where the spatially averaged neck velocity is identified to the external acoustic velocity. Therefore, we add a porosity factor $S_n/S_b$ to $u_n$ and obtain

$$v_{\mathrm{ex}}=\frac{S_n}{S_b}u_n. \tag{42}$$

Then we have to define what we mean with impedance for a sound field that is not entirely harmonic anymore. The natural choice is to define the impedance as the ratio of the Fourier transforms of the external pressure $p_{\mathrm{ex}}$ and (minus) the external velocity $v_{\mathrm{ex}}$ at excitation frequency $\omega$.

$$Z(\eta)=\frac{\hat{p}_{\mathrm{ex}}(\eta)}{-\hat{v}_{\mathrm{ex}}(\eta)}=\frac{\frac{1}{2\pi}\int_{-\infty}^{\infty}p_{\mathrm{ex}}(t)\mathrm{e}^{-\mathrm{i}\eta t}\,\mathrm{d}t}{-\frac{1}{2\pi}\int_{-\infty}^{\infty}v_{\mathrm{ex}}(t)\mathrm{e}^{-\mathrm{i}\eta t}\,\mathrm{d}t}\quad(\eta=\omega). \tag{43}$$

### 5.1. Non-resonant impedance

Taking the Fourier transforms of $p_{\mathrm{ex}}$ and $v_{\mathrm{ex}}$, we have, from (14), (8), and (10), for $\eta>0$

$$\hat{p}_{\mathrm{ex}}(\eta)=\frac{1}{2\pi}\int_{-\infty}^{\infty}p_{\mathrm{ex}}(t)\mathrm{e}^{-\mathrm{i}\eta t}\,\mathrm{d}t=\varepsilon^2\rho_0c_0^2\frac{\ell S_n}{V}F_0\delta(\eta-\omega) \tag{44}$$

and

$$\hat{v}_{\mathrm{ex}}(\eta)=\frac{1}{2\pi}\int_{-\infty}^{\infty}v_{\mathrm{ex}}(t)\mathrm{e}^{-\mathrm{i}\eta t}\,\mathrm{d}t=-\frac{S_n}{S_b}\varepsilon\omega\ell\left[-\varepsilon\frac{F_0}{1-\Omega^2}\frac{1}{\mathrm{i}}\delta(\eta-\omega)+\varepsilon^2\frac{rF_0\Omega}{(1-\Omega^2)^2}\delta(\eta-\omega)\right], \tag{45}$$

and so (with $V=LS_b$) we obtain

$$Z(\omega)=-\frac{\hat{p}_{\mathrm{ex}}(\omega)}{\hat{v}_{\mathrm{ex}}(\omega)}=\frac{\varepsilon\rho_0c_0^2}{L\omega}\cdot\left(\frac{\varepsilon^2r\Omega}{(1-\Omega^2)^2}+\mathrm{i}\frac{\varepsilon}{1-\Omega^2}\right)^{-1}. \tag{46}$$

To leading order in $\varepsilon$, we obtain the usual expression for the linear impedance as

$$Z(\omega)\simeq\frac{S_b}{S_n}\left(R+\mathrm{i}\rho_0\ell\omega_0\left(\frac{\omega}{\omega_0}-\frac{\omega_0}{\omega}\right)\right). \tag{47}$$

### 5.2. Resonant impedance

Taking the Fourier transforms of $p_{\mathrm{ex}}$ and $v_{\mathrm{ex}}$, we have for $\eta>0$

$$\hat{p}_{\mathrm{ex}}(\eta)=\frac{1}{2\pi}\int_{-\infty}^{\infty}p_{\mathrm{ex}}(t)\mathrm{e}^{-\mathrm{i}\eta t}\,\mathrm{d}t=\varepsilon^2\rho_0c_0^2\frac{\ell S_n}{V}F_0\delta(\eta-\omega) \tag{48}$$

and

$$\hat{v}_{\rm ex}(\eta)=\frac{1}{2\pi}\int_{-\infty}^{\infty} v_{\rm ex}(t)\mathrm{e}^{-\mathrm{i}\eta t}\,\mathrm{d}t=\frac{S_n}{S_b}\varepsilon\omega\ell\mathrm{e}^{-\mathrm{i}\theta}\left[-\mathrm{i}(A_0+\varepsilon A_1)\delta(\eta-\omega)+\frac{2}{9\pi}\varepsilon A_0|A_0|\delta(\eta-\omega)-\frac{1}{4\pi}\varepsilon A_0|A_0|\sum_{n=1}^{\infty}\frac{(2n+1)\delta(\eta-(2n+1)\omega)}{n(n+1)(n^2-\frac{1}{4})(n+\frac{3}{2})}+\cdots\right], \tag{49}$$

and so (with $V=LS_b$) we obtain

$$Z(\omega)=-\frac{\hat{p}_{\rm ex}(\omega)}{\hat{v}_{\rm ex}(\omega)}=\frac{\varepsilon\rho_0c_0^2F_0}{L\omega}\cdot\frac{-\mathrm{i}\mathrm{e}^{\mathrm{i}\theta}}{A_0+\varepsilon A_1+\mathrm{i}\frac{2}{9\pi}\varepsilon A_0|A_0|}. \tag{50}$$

It is interesting to consider $Z$ to leading order in $\varepsilon$

$$Z(\omega)\simeq\frac{\varepsilon\rho_0c_0^2F_0}{L\omega}\frac{-\mathrm{i}\mathrm{e}^{\mathrm{i}\theta_0}}{A_0}=\rho_0c_0\frac{c_0}{\omega L}\left(\frac{R}{\rho_0\omega_0\ell}+\frac{4}{3\pi}\frac{\|u_n\|}{\omega\ell}+2\mathrm{i}\frac{\omega-\omega_0}{\omega_0}\right) \tag{51}$$

(where $\|u_n\|$ denotes the amplitude of $u_n$) and observe that indeed Re($Z$) is of the often assumed form $a+b\|u_n\|$. Although our $a$ and $b$ are not constants and depend on $\omega$, this is a higher order effect because $\omega=\omega_0(1+O(\varepsilon))$. To leading order in $\varepsilon$ they are constant. Im($Z$) is independent of the excitation amplitude.

In order to illustrate formula (50), we have plotted in Fig. 5 resistance Re($Z$) and reactance Im($Z$) as a function of $\Omega$, obtained for a typical geometry at different driving amplitudes, corresponding with $\varepsilon$ varying from 0.05 to 0.28. As may be expected from (51), the main effect of the forcing amplitude is in the resistance. The reactance is practically independent of it. Typically, the resistance, being highest at or near the resonance frequency and decaying along both sides, increases everywhere with the amplitude, but more for frequencies less than resonance.

### 5.3. Comparison with Motsinger and Kraft [12]

The behaviour in (50) may be compared in Fig. 6 with the measurements and predictions given by Motsinger and Kraft in [12]. Their predictions are (a.o.) based on a resistance of the form $R=\rho_0c_0(a+b|v|)$ with suitably chosen $a$ and $b$. Unfortunately, only little experimental data for the higher amplitudes are available. The parameter values we used are based on $\omega_0/2\pi=2200$ Hz, $\ell=0.001$ m, $L=0.035$ m, $S_n/S_b=0.05$, $r=0.1$.

The agreement is reasonable, taking into account that the $\varepsilon$'s are not very small and no experimental data are available in this frequency range for the higher amplitudes. Especially the increase of the maximum with the amplitude is confirmed. Only for the higher amplitudes (with value of $\varepsilon=0.99$ or higher, that is far beyond what could be considered asymptotically "small") and frequencies well above resonance the decay suggested by [12] is not confirmed.

### 5.4. Comparison with Hersh et al. measurements [3]

The Hersh et al. model [3] to predict the impedance is based on the experimental calibration of empirical parameters that were derived in the formulation. They introduced six assumptions, mostly inspired from measurements, to model the nonlinear terms. Shown in Fig. 7 is the comparison of our non-resonant and resonant impedance values with two model

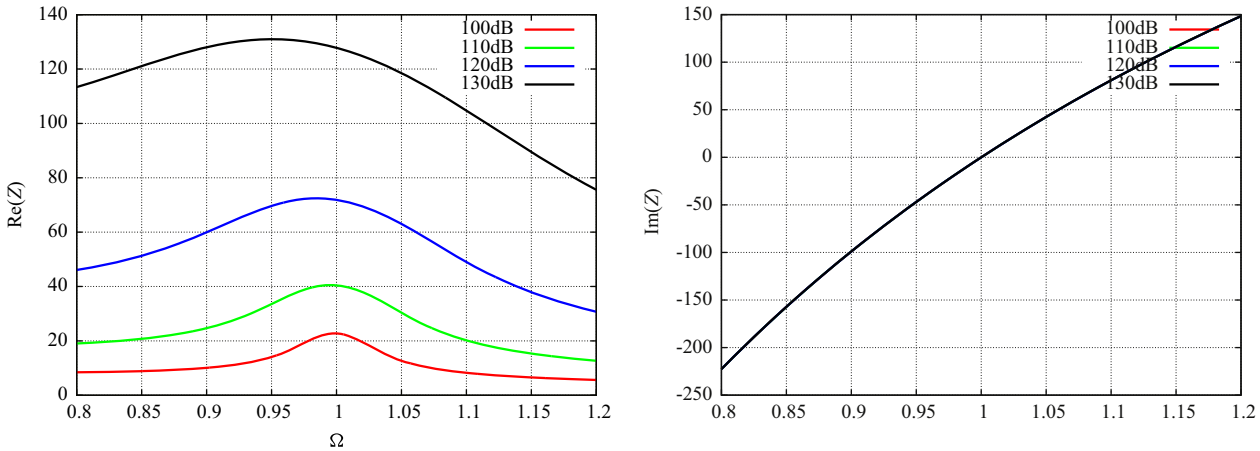


| $p_{ex}$ (dB) | 100 | 110 | 120 | 130 |
|---|---|---|---|---|
| $\varepsilon$ | 0.0497 | 0.0884 | 0.1572 | 0.2796 |

**Fig. 5.** Real and imaginary parts of impedance $Z$ for a Helmholtz resonator as a function of nondimensional frequency at different driving amplitudes. The realistic configuration that is chosen corresponds with $S_n/S_b=0.05$, $r=0.2$, $\omega_0/2\pi=1447$ Hz, $L=0.035$ m, $\ell=0.002$ m.

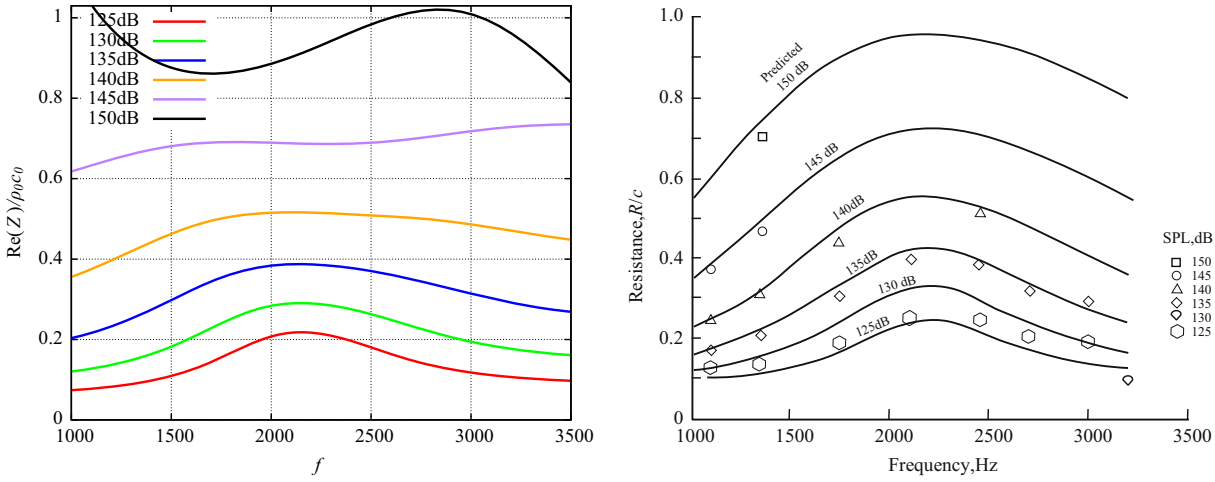


| $p_{ex}$ (dB) | 125 | 130 | 135 | 140 | 145 | 150 |
|---|---|---|---|---|---|---|
| $\varepsilon$ | 0.3125 | 0.4168 | 0.5558 | 0.7411 | 0.9883 | 1.3179 |

**Fig. 6.** Comparison of (50) with measurements and predictions of $\mathrm{Re}(Z)/\rho_0 c_0$ given in [12]. The markers in the right figure represent the measured values which were used, by adopting the relation $R=\rho_0 c_0(a+b|v|)$, to predict the resistance in solid curves.

configurations which have different values of $\ell$. The maximum of 120 dB curve was used for calibration and find $r$, and the same value of $r$ was used for other amplitudes. The nonlinear curves asymptotically match with the linear curve and this transition is quite smooth for lower $\varepsilon$ such that we can go from one model to the other. The resistance compares nicely at the near resonance frequencies when $\sigma=O(1)$ with one amplitude fitted. Away from resonance ($\varepsilon\sigma=O(1)$) we see a considerable overprediction of the resistance. The reactance shows a good comparison across the range of frequencies. The same comparison was done with other experimental configurations from [3] and a reasonably good agreement is found for the near resonance frequencies.

### 5.5. Comparison with Ingard and Ising [22]

Ingard and Ising [22] measured simultaneously fluctuating velocity and pressure, using hot wire measurements, followed by the exploitation of their phase relation to obtain the impedance at relatively high amplitudes. The chosen amplitudes were relatively high and in the domain of the Innes and Crighton theoretical model [11]. The comparison shown in Fig. 8 is very accurate. This is a fortuitous result because we cannot expect correct behaviour of the asymptotic analysis at such high $\varepsilon=O(1)$. It is a general observation that the predicted impedance in the close neighbourhood of resonance frequency is always agreeable even with higher values of $\varepsilon$.

### 5.6. Comparison with Melling [21]

The measurements of Melling were used to further validate the model. Melling measured the impedance of a series of resonators constructed with multiple orifices backed by a cavity. Fig. 9 shows that the model predicted nonlinear resistance of a resonator constructed with an orifice diameter $(4S_n/\pi)^{1/2}=0.127$ cm, $\ell=0.056$ cm, $L=7.5$ cm and $(S_b/\pi)^{1/2}=3.46(S_n/\pi)^{(1/2)}$ cm. The value of $r$ is calibrated by its value giving the 143.5 dB amplitude. The first three points of the measurements, being equal in magnitude, are apparently in the linear (non-resonant) range. The model prediction is quite reasonable over the full amplitude regime.

### 5.7. Comparison of impedances based on $y_0$ and $y_0+\varepsilon y_1$ approximations

It is of interest to know when the driving amplitude becomes large enough to warrant the extra term $\varepsilon y_1$ in the approximation of $Z$. Shown in Fig. 10 is the comparison of the impedance values obtained from $y_0$ and $y_0+\varepsilon y_1$ approximations for different values of $\varepsilon$. Taking the same realistic geometry as above (Fig. 5), the value of $\varepsilon$ varies from $\sim 0.05$ to 0.28 as the external driving amplitude is changed from 100 dB to 130 dB. We see that $O(\varepsilon)$ correction in the resulting resistance (the reactance is practically independent, especially near resonance) can be neglected for the lower amplitudes, but is indeed essential for the higher amplitudes.

## 6. Conclusions

A systematic approximation of the hydrodynamically nonlinear Helmholtz resonator equation is obtained, including the resulting impedance if the resonator is applied in an acoustic liner. To leading order, the usually assumed form of the

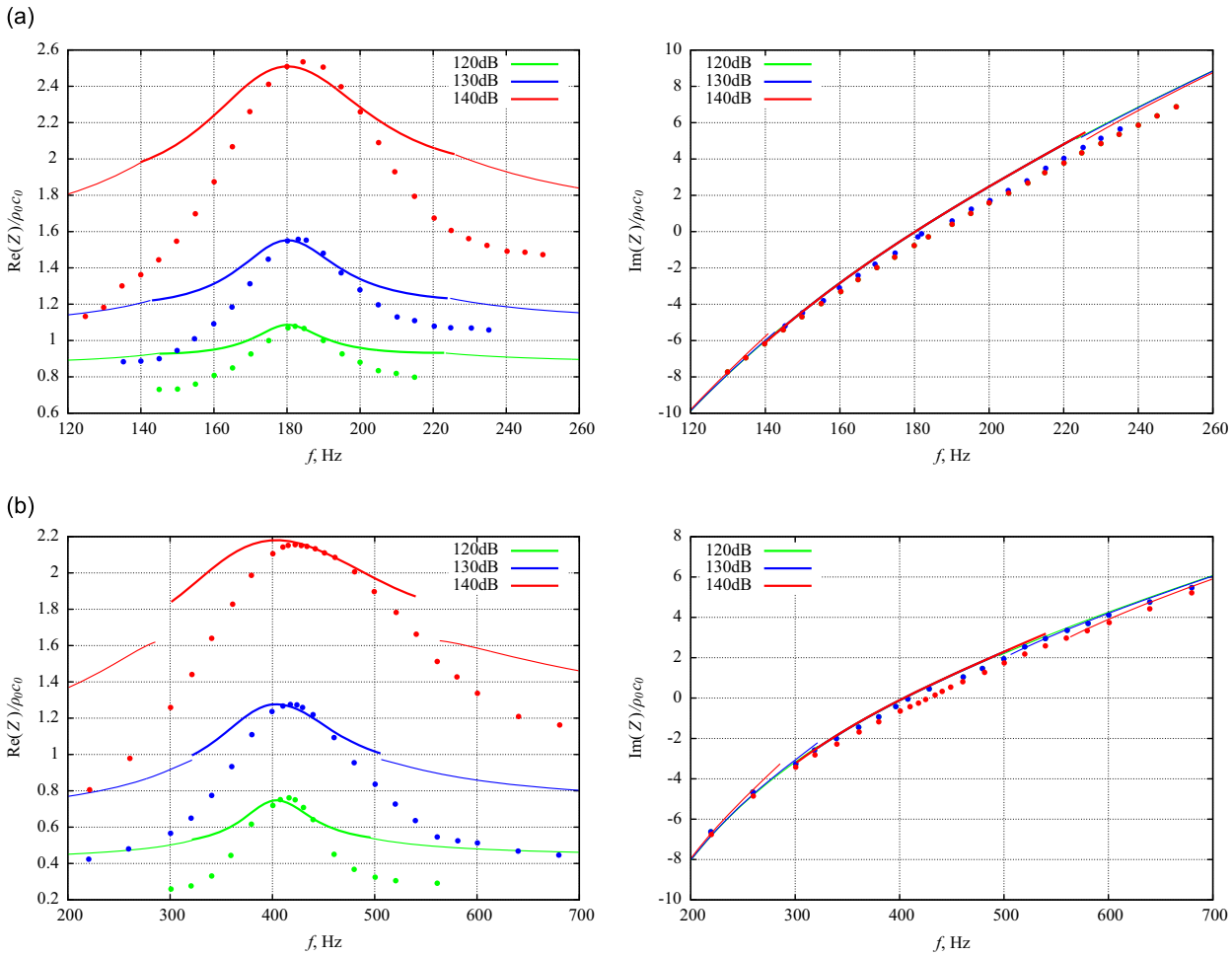


**Fig. 7.** Comparison of the resonant (—) and non-resonant (−) resistance with Hersh and Walker measurements (···). (a) *Configuration* 1: The cavity parameters are $\ell = 5.08$ cm, $(4S_n/\pi)^{1/2} = 0.635$ cm, $L = 2.54$ cm and $(4S_b/\pi)^{1/2} = 5.08$ cm. The desired resistance is obtained for $r = 0.65$. Amplitudes 120, 130, 140 dB correspond with $\epsilon = 0.0455, 0.0809$ and $0.1439$. (b) *Configuration* 2: The cavity parameters are $\ell = 0.635$ cm, $(4S_n/\pi)^{1/2} = 0.635$ cm, $L = 2.54$ cm and $(4S_b/\pi)^{1/2} = 5.08$ cm. The desired resistance is obtained for $r = 1$. Amplitudes 120, 130, 140 dB correspond with $\epsilon = 0.1021, 0.1815$ and $0.3228$.

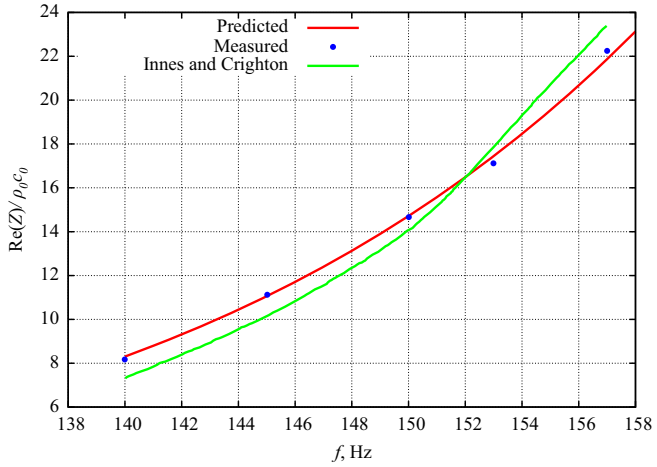


**Fig. 8.** Comparison of the resistance with the measurements of Ingard and Ising. The cavity parameters are $\ell = 0.01$ cm, $(4S_n/\pi)^{1/2} = 0.7$ cm, $L = 7.5$ cm and $(4S_b/\pi)^{1/2} = 9.5$ cm. The desired resistance is obtained for $r = 1$. $1.37541 < \varepsilon < 3.87643$.

resistance, $a + b|v|$, is recovered. The only unknown parameter that we need to adapt is resistance factor $r$, although in many cases the effective neck length $\ell$ is also unknown and has to be estimated. Comparisons with measurements prove that the model predicts the near resonance impedance at $\sigma = O(1)$ to a good accuracy.

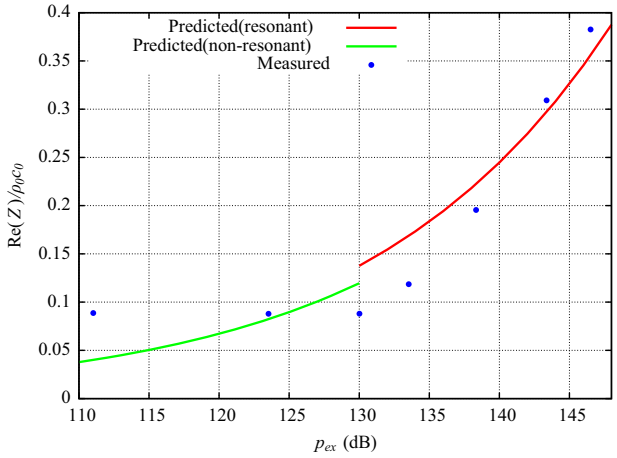


**Fig. 9.** Comparison of the resistance with the measurements of Melling. The cavity parameters are $\ell = 0.056$ cm, $(4S_n/\pi)^{1/2} = 0.127$ cm, $L = 7.5$ cm and $(S_b/\pi)^{1/2} = 3.46(S_n/\pi)^{1/2}$ cm. The desired resistance is obtained for $r = 1$. $0.0705516 < \varepsilon < 0.705516$.

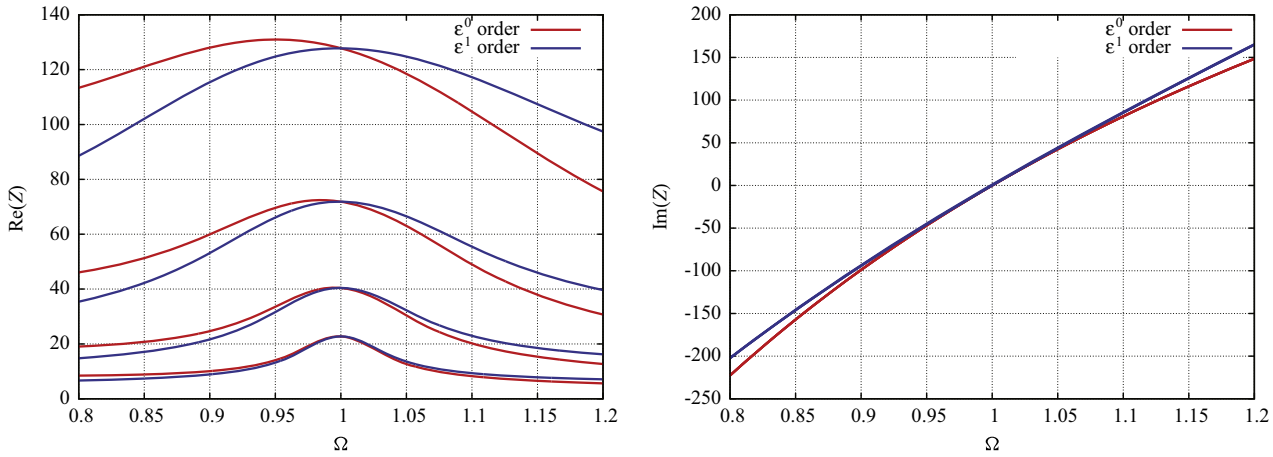


**Fig. 10.** Comparison of the impedance obtained from the $y_0$ and $y_0 + \epsilon y_1$ approximations for 100 dB, 110 dB, 120 dB and 130 dB. Same configuration as in Fig. 5.

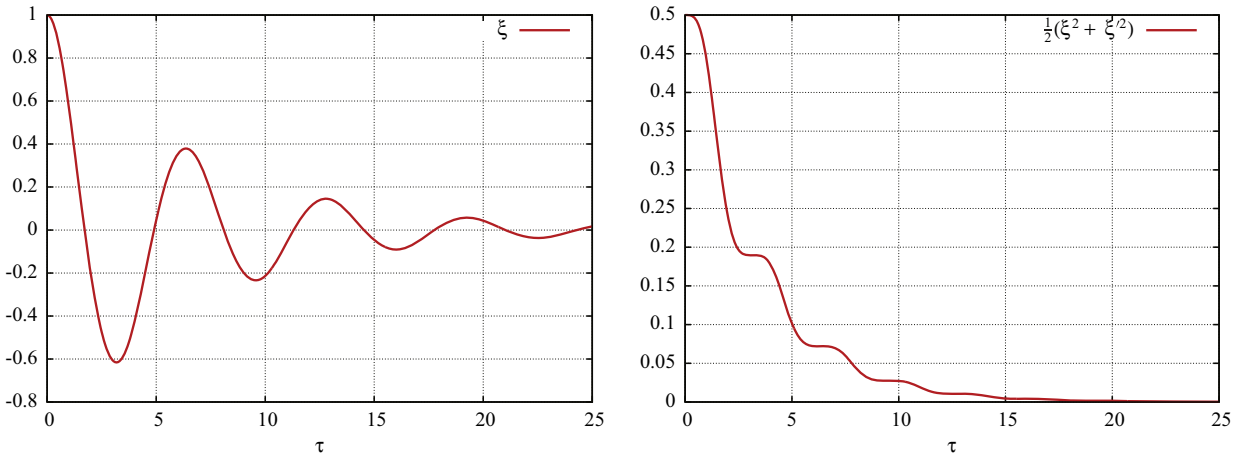


**Fig. 11.** Amplitude $\xi$ and mechanical energy $\frac{1}{2}(\xi^2 + \xi'^2)$ of a superimposed perturbation when it starts from $\xi(0) = 1$ $\xi'(0) = 0$. The full solution was approximated by $y = A_0 \cos(\Omega\tau)$ with $\varepsilon = 0.16$, $\Omega = 1$ and $r = 0.2$.

Our approach, based on the systematic use of asymptotic analysis, allows higher order corrections, which indeed are shown to be important and relevant for practical configurations involving high amplitudes.

The real part of the found impedance (the resistance) shows the usual characteristic behaviour as a function of frequency, namely a maximum at or near the resonance frequency and a decay along both sides. All values increase with the amplitude,

but slightly more for the frequencies less than resonance. The imaginary part of the impedance (the reactance) is linear in frequency in a way that it vanishes at resonance and is practically independent of the amplitude.

## Acknowledgements

A preliminary version of this work was presented as paper AIAA-2013-2223 at the 19th AIAA/CEAS Aeroacoustics Conference, Berlin.

We gratefully acknowledge the support from the European Union through ITN-project *FlowAirS* (Contract no. FP7-PEOPLE-2011-ITN-289352), with coordinator Yves Aurégan.

## Appendix A. Stability of stationary solution

From the physical origin of the problem, it is very likely that there exists a stable steady solution for a steady external forcing, such that we are not approximating a solution that just would not exist in any realisation. We have checked this mathematically by proving the boundedness of a small perturbation $\xi$ of our solution $y$ in (13), satisfying the following equation:

$$(y''+\xi'')+\varepsilon(y'+\xi')|y'+\xi'|+\varepsilon r(y'+\xi')+(y+\xi)=\varepsilon F(\tau). \tag{52}$$

Since, by assumption, $y$ is any solution of the original equation, we have to linear order for small $\xi$ (and a slight error near the zeros of $y'+\xi'$)

$$\xi''+\phi(\tau)\xi'+\xi=0 \tag{53}$$

where $\phi(\tau)=\varepsilon(r+2|y'|)\geq 0$ (even strictly positive if $r>0$). We assume an initial condition with $\xi(0)^2+\xi'(0)^2=E_0^2$. From (53) we have for the mechanical energy $\frac{1}{2}(\xi^2+\xi'^2)$

$$\frac{\mathrm{d}}{\mathrm{d}\tau}\left(\frac{1}{2}(\xi^2+\xi'^2)\right)=\xi'\xi''+\xi'\xi=-\phi\xi'^2\leq-\phi(\xi^2+\xi'^2).$$

It follows that $(\mathrm{d}/\mathrm{d}\tau)\ln(\xi^2+\xi'^2)\leq-2\phi$. After integration and using the positivity of $\phi$we find eventually

$$\xi^2+\xi'^2\leq E_0^2\exp\left(-2\int_0^\tau\phi(\tau)\,\mathrm{d}\tau\right).$$

Hence it follows that perturbations are bounded and will decay to zero, confirming the existence of a stable stationary solution. Shown in Fig. 11 is a plot of $\xi$ and $\frac{1}{2}(\xi^2+\xi'^2)$.

## References

[1] A. Cummings, W. Eversman, High amplitude acoustic transmission through duct terminations theory, *Journal of Sound and Vibration* 91 (4) (1983) 503–518.
[2] A. McAlpine, M.J. Fisher, B.J. Tester, Buzz-saw noise a comparison of modal measurements with an improved prediction method, *Journal of Sound and Vibration* 306 (3–5) (2007) 419–443.
[3] A.S. Hersh, B.E. Walker, J.W. Celano, Helmholtz resonator impedance model, part 1 nonlinear behavior, *AIAA Journal* 41 (5) (2003) 795–808.
[4] A.W. Guess, Calculation of perforated plate liner parameters from specified acoustic resistance and reactance, *Journal of Sound and Vibration* 40 (1) (1975) 119–137.
[5] B.T. Zinn, A theoretical study of non-linear damping by Helmholtz resonators, *Journal of Sound and Vibration* 3 (1970) 347–356.
[6] C. Bréard, A. Sayma, M. Imregun, A.G. Wilson, B.J. Tester, A CFD-based non-linear model for the prediction of tone noise in lined ducts. *The 7th AIAA/CEAS Aeroacoustics Conference*, AIAA-2001-2176, 2001.
[7] C.K.W. Tam, H. Ju, M.G. Jones, T.L. Parrott, A computational and experimental study of slit resonators, *Journal of Sound and Vibration* 284 (2005) 947–984.
[8] C.K.W. Tam, H. Ju, M.G. Jones, W.R. Watson, T.L. Parrott, A computational and experimental study of resonators in three dimensions, *The 15th AIAA/CEAS Aeroacoustics Conference*, AIAA Paper 2009-3173, 2009.
[9] C.K.W. Tam, K.A. Kurbatskii, Microfluid dynamics and acoustics of resonant liners, *AIAA Journal* 38 (8) (2000) 1331–1339.
[10] C.K.W. Tam, K.A. Kurbatskii, K.K. Ahuja, R.J. Gaeta Jr., A numerical and experimental investigation of the dissipation mechanisms of resonant acoustic liners, *Journal of Sound and Vibration* 245 (3) (2001) 545–557.
[11] D. Innes, D.G. Crighton, On a non-linear differential equation modelling Helmholtz resonator response, *Journal of Sound and Vibration* 131 (2) (1989) 323–330.
[12] H.H. Hubbard, Acoustical Society of America, Aeroacoustics of flight vehicles: noise sources, *Aeroacoustics of Flight Vehicles: Theory and Practice, Vol. 1: Noise Sources; Vol. 2: Noise Control*, Published for the Acoustical Society of America through the American Institute of Physics.
[13] A.S. Hersh, B. Walker, Effect of Grazing Flow on the Acoustic Impedance of Helmholtz Resonators Consisting of Single and Clustered Orifices, NASA Contractor Report 3177, 1979.
[14] U. Ingard, On the theory and design of acoustic resonators, *Journal of The Acoustical Society of America* (1953) 25.
[15] J.H.M. Disselhorst, L. van Wijngaarden, Flow in the exit of open pipes during acoustic resonance, *Journal of Fluid Mechanics* 99 (2) (1980) 293–319.
[16] J.M. Roche, L. Leylekian, G. Delattre, F. Vuillot, Aircraft fan noise absorption: DNS of the acoustic dissipation of resonant liners, *The 15th AIAA/CEAS Aeroacoustics Conference*, AIAA Paper 2009-3146, 2009.
[17] Q. Zhang, D.J. Bodony, Numerical simulation of two-dimensional acoustic liners with high speed grazing flow, *AIAA Journal* 49 (2) (2011) 365–382.
[18] R.E. Mickens, *An Introduction to Nonlinear Oscillations*, Cambridge University Press, 1981.
[19] R.M.M. Mattheij, S.W. Rienstra, J.H.M. ten Thije Boonkkamp, *Partial Differential Equations: Modeling, Analysis, Computation*, Society for Industrial and Applied Mathematics, 2005.

[20] S.W. Rienstra, A. Hirschberg, An Introduction to Acoustics, Technical Report, Technische Universiteit Eindhoven, Revised and updated version of IWDE 92-06, ⟨http://www.win.tue.nl/∼sjoerdr/papers/boek.pdf⟩, 2012.
[21] T.H. Melling, The acoustic impedance of perforates at medium and high sound pressure levels, *Journal of Sound and Vibration* 29 (1) (1973) 1–65.
[22] U. Ingard, H. Ising, Acoustic nonlinearity of an orifice, *Journal of the Acoustical Society of America* 42 (1) (1967) 6–17.
[23] U. Ingard, S. Labate, Acoustic circulation effects and the nonlinear impedance of orifices, *Journal of Acoustic Society of America* 22 (1950) 211–219.